Nanomaterials and Nanotechnology

OPEN ACCESS
ARTICLE

ZnO Tetrapods: Synthesis and Applications in Solar Cells

Review Article

Luting Yan[1,2]*, Ashraf Uddin[2] and Haiwei Wang[1]

1 School of Science, Beijing Jiaotong University, Beijing, PR China
2 School of Photovoltaics and Renewable Energy Engineering, University of New South Wales, Sydney, Australia
*Corresponding author(s) E-mail: ltyan@bjtu.edu.cn

Received 19 February 2015; Accepted 29 May 2015

DOI: 10.5772/60939

Abstract

Zinc oxide (ZnO) tetrapods have received much interest due to their unique morphology, that is, four arms connected to one centre. Tetrapod networks possess the excellent electronic properties of the ZnO semiconductor, which is attractive for photoelectrode materials in energy-conversion devices because of their advantages in electron extraction and transportation. In this review, we have discussed recent advancements in the field of ZnO tetrapod synthesis, including vapour transport synthesis and the wet chemical method, together with their advantages and disadvantages in terms of morphology control and yield regulation. The developments and improvements in the applications of ZnO nanotetrapods in photovoltaics, including dye-sensitized solar cells and polymer solar cells, are also described. Our aim is to give readers a comprehensive and critical overview of this unique morphology of ZnO, including synthesis control and growth mechanism, and to understand the role of this particular morphology in the development of solar cells. The future research directions in ZnO tetrapods-based solar cell are also discussed.

Keywords ZnO tetrapods, synthesis, application, photovoltaic

1. Introduction

Zinc Oxide (ZnO) is an important and versatile n-type direct wide bandgap (3.37 eV) semiconductor, with a large exciton-binding energy (~60 meV) at room temperature. ZnO has wide-ranging applications in electronic and optoelectronic devices, such as piezoelectric sensors, ultraviolet (UV)/blue light-emitting diodes, transistors, field emission displays, gas sensors, UV detectors, transparent conductive films, hybrid solar cells, etc. ZnO is also inexpensive, relatively abundant, chemically stable, easy to prepare, and nontoxic [1, 2] In addition, ZnO is amenable to processing into variegated morphologies in terms of nanostructure synthesis, owing to its hexagonal wurtzeit (WZ) crystal structure and different growth rates of the diverse crystal planes. To date, a variety of morphologies have been achieved, including nanopowders, nanobelts, nanobows, nanodiscs, nanoplatelets, nanoflowers, nanowires, nanotetrapods and nanorods [3-5]. These novel nanostructures indicate that ZnO contains probably the richest family of nanostructures among all materials, in both structure and properties, as well as providing valuable models for understanding crystal-growth mechanisms at nanosize, and exhibiting high potential for fabricating novel nanoelectronics and optical devices with enhanced performance [6]. Among the various morphologies of ZnO

nanostructures, ZnO tetrapods have recently attracted extensive attention due to their unique shape and structure, excellent optical properties and significantly lower density of native defects when compared to other morphologies [7]. A ZnO tetrapod consists of a ZnO core from which four arms extend to the surrounding space at the same extent, which endows them with the ability to assemble a good network with desired the porosity and mechanical strength by connecting arms with each other. This material is often used as a reinforcing material in composite materials [8, 9], and it has already proved to have promising applications in biomedical engineering and advanced linking technologies [10, 11]. The electron mobility is ~17 cm^2 V^{-1} s^{-1} for single-crystal ZnO nanowires, and it is similar in ZnO tetrapods [12]. The bandgap energy and the electron affinities of ZnO are similar to TiO_2, but its higher electron mobility compared to TiO_2 may overcome higher electron recombination in the TiO_2-based dye sensitized solar cells (DSSCs), which is beneficial for solar cell performance. The ZnO porous networks are superior in providing electron extraction to one-dimensional (1D) nanorod structures or bulk materials as interconnections and functional components in photovoltaic devices [13-17], because nanotetrapods can always transport electrons in the direction perpendicular to the conductive substrate by directing the constituent arms in the four tetrahedral directions. The porous networks are also important in increasing the diffusion rate without increasing the recombination rate, and could therefore increase the efficiency of a photoelectrochemical energy conversion system. Tetrapod nanocrystals have also been used successfully in hybrid solar cells due to their unique, continuous pathway, controllable absorption maximum and semiconducting properties [18]. Improved efficiencies, when compared with polymer-based structures, are found to result from enhanced electron-extraction because of the branched tetrapods. Researchers have seen potential in ZnO tetrapods for solar cell applications owing to their vectorial charge transportation, excellent charge collection and low temperature film formation process. The application of ZnO tetrapods in solar cells, therefore, would be interesting.

Controlled synthesis of ZnO tetrapods is one of the most important issues for their successful application in solar cells. The arm length-to-diameter ratio has a great influence on the packing density of the tetrapods, which determine the interface charge separation as well as the electron transport in solar cells. ZnO tetrapods have been synthesized by various methods, such as carbothermal reduction, atmosphere controlled oxidation, the microwave plasma method, the hydrothermal method or the simple method of heating ZnO powders with or without a catalyst. This review presents recent advances in usage of ZnO tetrapods, especially focusing on the synthesis methods, including their advantages and disadvantages in terms of morphology control and yield regulation, the growth mechanisms and their application in photovoltaic devices. Future research directions in ZnO tetrapods-based solar cells are also discussed.

2. Synthesis Methods

As in other ZnO nanostructures' synthesis [19-24], ZnO tetrapods can be obtained via different methods [25-27], such as atmosphere controlled oxidation, thermal evaporation, catalytic oxidation, microwave radiation, and microemulsion. All these methods can be divided into two primary categories: the first starts from a solid phase and then proceeds through a solid–vapour transport–condensation process, while the second is a liquid reaction process.

2.1 Vapour transport synthesis

The vapour transport process is widely used to synthesize ZnO tetrapods due to its simplicity, low cost, high yield, and lack of agglomeration. The vapour transport synthesis undergoes the evaporation of Zn metal, oxidation, nucleation and growth, all of which take place at high temperatures (> 600 °C). The tetrapods, once nucleated, would grow rapidly in the high-temperature region and turn into exclusively large sizes. ZnO tetrapods obtained through vapour transport synthesis normally have arm diameters larger than 100 nm and arm lengths larger than 2 μm. The important process parameters in vapour transport reactions are the partial pressures of reactant gases, growth temperature and particle size of the nuclei [28-30]. Although it has a common solid-gas-solid changing experience, the vapour transport synthesis also includes different subclasses, owing to the specific experimental parameters and the different raw materials. We placed emphasis on thermal evaporation, atmosphere-controlled oxidation, carbothermal reduction, catalytic oxidation, thermal oxidation combined with a solution and the microwave plasma method.

2.1.1 Thermal evaporation

Zinc powder is directly placed into a reactor for thermal evaporation and oxidation. No catalyst is needed in this process, and the reaction atmosphere in the reactor need not be controlled. The amount of zinc powder is calculated according to the volume of the reactor, while ensuring some oxygen insufficiency in the reactor.

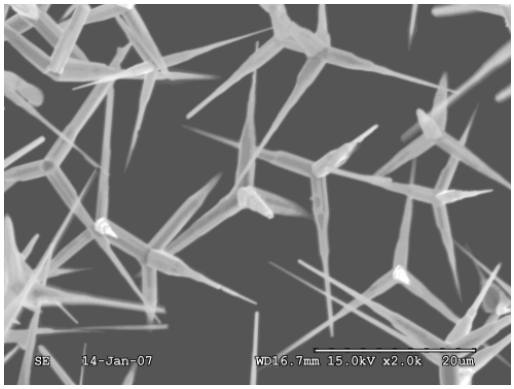

Figure 1. SEM image of ZnO tetrapods by thermal evaporation [31]

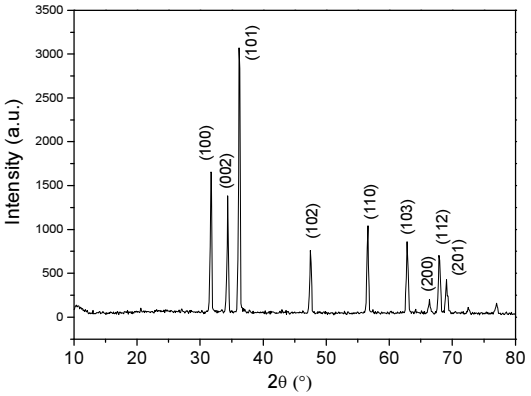

Figure 2. XRD patterns of ZnO tetrapods grown by thermal evaporation [31]

Figure 1 shows the SEM images and Figure 2 shows the XRD patterns of ZnO tetrapods [31]. From Figure 1 we can see that the tetrapods consist of four arms branching from the same centre and that the angles between the arms are nearly the same, analogous to the spatial structure of molecular methane. The four arms of the ZnO tetrapod gradually become thinner from their widest point at the centre (about 1-2 μm in diameter) and eventually end in needle-shaped tips (about 40 nm in diameter). They are usually several to tens of microns in length. All the diffraction peaks in Figure 2 can be indexed as a wurtzeit structure with lattice constants of a = 0.324 nm and c = 0.519 nm. ZnO tetrapods prepared by thermal evaporation have optimal morphology with high crystal quality. However, the size of ZnO tetrapods obtained using this method is within the micron range. The growth of ZnO whiskers is mainly determined by two factors: one is the supersaturation of ZnO above the substrates, and the other is the crystallization property of the ZnO material itself. The supersaturation of ZnO is the most important parameter and can be regulated by controlling the temperature and reaction rate. In reference [31], the heating process is divided into three stages: a preheating stage to 700 °C, a heating stage to the reaction temperature, and a heat preservation stage at the reaction temperature for some time. The experimental results show that at a low preheating rate of 3 °C/min, the morphology of ZnO tetrapods is optimal and the yield is as high as 95%. With an increased preheating rate, the size of the tetrapod product increases and becomes uneven. With the increased reaction temperature exceeding 1000 °C, the whisker size, yields and integrity decrease.

In the thermal evaporation process, tetrapods, once nucleated, grow rapidly in the high-temperature region. This dramatic growth can be quenched in a controlled manner, i.e., the size and morphology of the tetrapods can be tailored. Qiu [32] developed a fast-flow technique to quench tetrapod growth by rapidly transporting the growing tetrapods with a flowing gas stream to the low-temperature region. With this simple technique, ZnO tetrapods with average arm diameters in the range of tens of nanometres and arm lengths ranging from 50 nm up to many micrometres can be obtained.

2.1.2 Atmosphere-controlled oxidation

One key step in the process of preparing ZnO tetrapods is controlling the oxidizing speed of zinc by forming homogeneous, thin, fine zinc oxide films on the surface of zinc particles to prevent zinc vapour from spreading out too fast and O_2 from penetrating the particles. To achieve this goal, ZnO tetrapods can be prepared in a mixed atmosphere of inert gas and oxygen gas. The diluted concentration of oxygen can then meet the conditions necessary for whisker generation. Carotta [33] heated metallic Zn foil to 650 °C under Ar gas flow. O_2 was then introduced to the Ar flow, and the furnace was cooled to room temperature. Large numbers of tetrapods were formed in the vapour phase and transported downstream in the colder area of the furnace.

The addition of water vapour to the reactive gas has a marked effect on the shape and size control of ZnO tetrapods. The tetrapods prepared with the addition of water have longer arms and a lower average diameter (8-20 nm) as compared to tetrapods prepared without water addition [34]. The reaction of Zn metal with water produces hydrogen gas that could favour the production of the suboxide of zinc, which has been reported as the most probable intermediate state in the formation of ZnO tetrapods [35, 36]. However, the reaction of zinc metal with excessive water results in the passivation of the surface stopping the transportation, thereby reducing the yield of ZnO. Thus, it appears that traces of water can be beneficial for the formation of ZnO tetrapods with controlled diameters, whereas larger water concentrations decrease the yield of ZnO considerably.

2.1.3 Carbothermal reduction

In the carbothermal method, ZnO powder is mixed with graphite powder as a source material. At about 800–1100 °C, graphite reduces ZnO to form Zn and CO/CO_2 vapours. Zn and CO/CO_2 subsequently react and form ZnO nanocrystals. The advantages of this method can be attributed to the ability of graphite to significantly lower the decomposition temperature of ZnO. Chen [37] reported ZnO tetrapods obtained through carbothermal reduction. A mixture of pure ZnO powder and graphite powder (1:1 molar ratio) as the starting material was placed in the centre of a quartz tube. The mixture was heated to approximately 1100°C under a flow of high-purity nitrogen as a carrier gas. Different products formed in different positions on the inner wall of the quartz tube when the flow rate of the carrier gas was adjusted. With an increased carrier gas flow rate to 50 sccm, uniform tetrapod-shaped ZnO crystals were formed on the inner wall of the quartz tube located downstream of the carrier gas by a distance of approximately 85–100 mm from the reactants. The growth temperature was estimated to range from 955°C to 990°C. Thus, the carrier-gas flow rate is a key parameter for controlling the formation of ZnO tetrapods by carbothermal reduction. A suitable gas flow

rate creates a moderate supersaturation of Zn vapour and oxygen, which leads to the formation of ZnO nanotetrapods.

2.1.4 Catalytic oxidation

By incorporating Pb, Cd, Sn, Al, Ag and Sb into pure Zn materials, ZnO tetrapods were formed after an oxidation process. The doping elements served as catalysts that altered the ZnO nucleation and growth processes of whiskers, leading to changes in the morphologies of ZnO [38]. Wang [39] used Au as a catalyst and produced a bulk quantity of tetrapod-like ZnO, which showed very similar structural features to those grown in a catalyst-free process.

ZnO nanostructures were synthesized by the thermal evaporation of ZnO and carbon nanotubes on a silicon substrate with a sputtered Ag catalyst [40]. For the samples with Ag catalysts, the yield of polypods was observed to be high (>95%), the majority of polypods were in tripod form and the remaining structures were mostly tetrapods. In the case of a no-catalyst layer, the majority of polypods were in tetrapod form and the size was relatively small. However, the density and production yield of polypods were relatively lower (< 50%) than was the case with an Ag catalyst layer. The experimental results showed that silver catalyst caused a significant change in polypod structure and yield. A plausible explanation is that use of the silver catalyst results in higher-density, larger-nucleated ZnO nanoparticles than those produced without a catalyst, because ZnO tripods and tetrapods prepared with the silver catalyst are relatively larger than ZnO nanotetrapods grown with no catalyst. In addition, ZnO nanoparticles nucleated on the silver catalyst have different crystal orientations from ZnO particles randomly nucleated on bare Si substrate, such that ZnO tripods are preferentially formed. By contrast, nanotetrapods are primarily grown from randomly nucleated ZnO particles on bare Si substrate.

2.1.5 Thermal oxidation combined with solution

In this process, ZnO tetrapods were prepared by the thermal oxidation technique of metal zinc powder mixed with different solutions such as methanol, ethanol and hydrogen peroxide in a 10:1 ratio. The mixtures were heated at 1000 °C in a normal atmosphere. The results showed that ZnO prepared by heating zinc and H_2O_2 yielded tetrapod-like nanostructures, and that H_2O_2 acted as a strong oxidizer that supplied more reactive oxygen species to zinc to form ZnO tetrapods [41].

2.1.6 Microwave plasma method

In a typical microwave radiation procedure, zinc powder in a quartz boat was set at the centre (the plasma heating zone) of a horizontal quartz tube. Pure Ar and O_2 gases flowed into the tube and a microwave source was coupled along a square or rectangular wave-conducting pipe to the tube's centre for generating stable plasma. An assistant tube furnace was used to provide the necessary temperature zone. Figure 3 shows a schematic illustration of a microwave plasma system. The products were collected on the inner wall at the downstream end of the tube. Zhang [42, 43] prepared ZnO tetrapods by a microwave plasma method. The obtained ZnO tetrapods had four straight and uniform legs with diameters ranging from 10 nm to 25 nm, and lengths up to 160 nm.

Among the vapour-transport synthesis methods, thermal evaporation under atmospheric pressure is the easiest, and ZnO tetrapods prepared by thermal evaporation have optimal morphology with high crystal quality. In general, the size of ZnO tetrapods obtained using this method is within the range of microns. However, ZnO tetrapods used in polymer-nanocrystal solar cells are within the order of 100 nm, and are generally much smaller than ZnO tetrapods fabricated by vapour deposition. This small size enables the formation of thin polymer layers that are required for efficient charge transport. Thus, although the vapour transporting process is the dominant synthesis method for growing ZnO tetrapods, liquid reaction processes have become increasingly important in forming ZnO tetrapods with arm diameters smaller than 100 nm and controlled arm lengths. These processes can fill important size gaps and significantly extend the applications of this unique nanostructure.

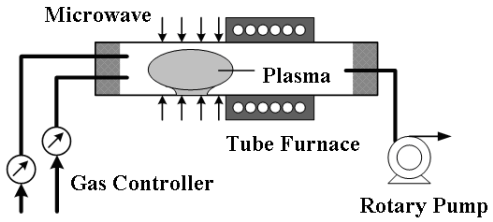

Figure 3. Schematic illustration of a microwave plasma system

2.2 Wet chemical method

Although the vapour transport process is the dominant synthesis method for growing ZnO tetrapods, other growth methods such as wet chemical methods have also been developed. These methods enable the formation of ZnO nanocrystals at low temperatures, which facilitates the formation of nanoscale ZnO tetrapods.

2.2.1 Micro-emulsion combined with the hydrothermal method

Micro-emulsion combined with thermal hydration can be used to prepare ZnO nanotetrapods because of its relative simplicity. This method is based on the advantages of microemulsion in producing fine particles, and of hydrothermal treatment in improving crystal morphology and quality [44]. In reference [45], $Zn(Ac)_2$ aqueous solution was added to a TritonX-100/cyclohexane/n-octanol system and stirred continuously to achieve a transparent solution. NaOH aqueous solution was added dropwise to the

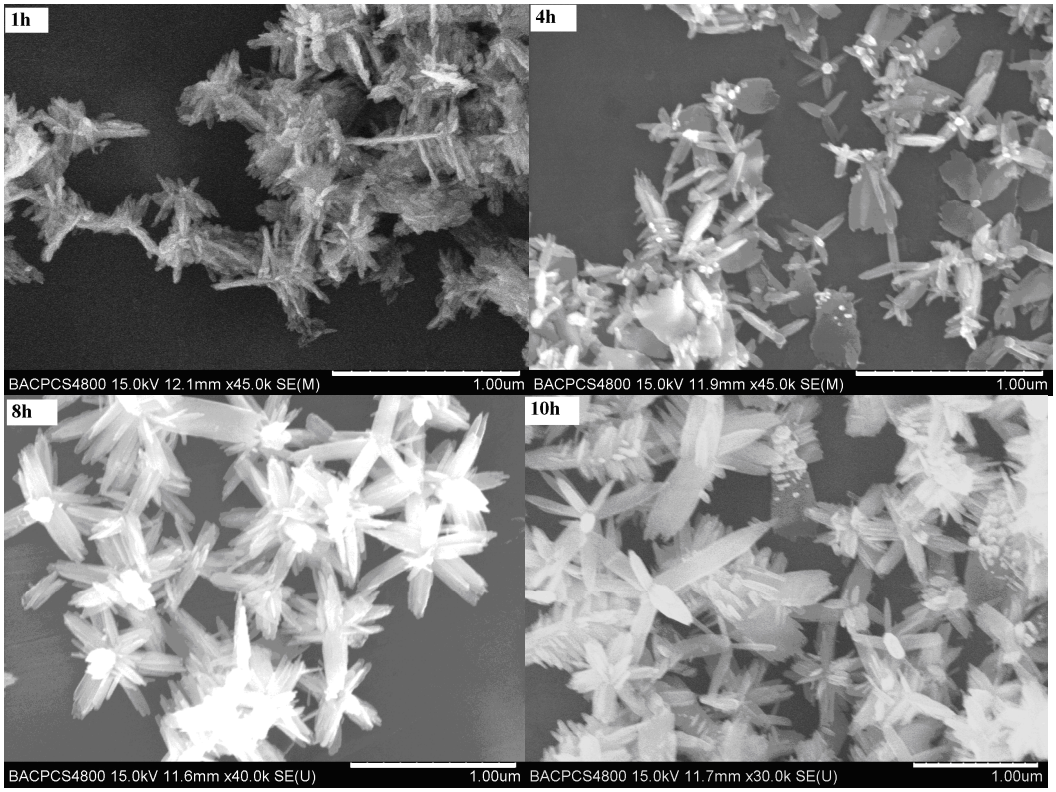

Figure 4. SEM images of as-synthesized ZnO whiskers under different growth times (TritonX-100/cyclohexane/n-octanol=3:8:2; water/cyclohexane=16:100) [45]

mixture, then the mixture was transferred to a hydrothermal autoclave for hydrothermal growth and the final product was collected by centrifugation. The hydrothermal growth time and cyclohexane dosage were studied to determine their effects on morphology and sizes.

Figure 4 shows the SEM images of ZnO whiskers prepared at different growth times. The ZnO products were mainly nanotetrapods. The lengths and diameters of tetrapods changed slightly over time. The ZnO whiskers prepared within a short growing time had nanotetrapod skeletons; however, numerous small particles were attached onto the arms. With growth time increased to four hours (h), the outline of the arms became clear and the crystals achieved a good growth. The main morphology of the whiskers was a nanotetrapod, apart from the sheet- and flower-shaped forms. With an increased growth time to eight h, a large number of flower-shaped whiskers appeared and the surface of the arm was no longer smooth. With a further increased growth time to 10 h, secondary growth occurred and numerous tiny whiskers appeared on the arms. This phenomenon shows the occurrence of polar growth and secondary growth during the crystal growth process, and that the growth time significantly affects the morphology of ZnO.

A possible growth mechanism for the formation of nano-ZnO by a microemulsion-mediated hydrothermal process was reported [46]. In the water-in-oil microemulsion, water droplets stabilized by the surfactant and co-surfactant were used as reactors for the formation of nanomaterials. The small size of the water core was a prerequisite favouring the formation of small particles, which was achieved by decreasing the amount of water or increasing the amount of oil. Figure 5 shows the SEM images of the as-synthesized ZnO whiskers under different water/cyclohexane ratios at a growth time of 10 h. The cyclohexane dosage exerted some influence on the size and morphology of ZnO whiskers. A slight increase in the cyclohexane dosage resulted in small-sized nanotetrapods. When the cyclohexane content reached a certain level, adding more cyclohexane resulted in a difficult dispersion. The viscosity increased and the microemulsion became a thermodynamically unstable system, which created some large-sized non-uniform ZnO whiskers.

2.2.2 Nonhydrolytic alcoholysis route

To further reduce the size of ZnO tetrapods, the alcoholysis of zinc stearate was attempted to prepare ZnO tetrapods <100 nm in size. Growth of ZnO nanocrystals through the reaction of zinc stearate with alcohol in hydrocarbon solvents (noncoordinating solvents) under elevated temperatures was chosen because the nanocrystals resulting in this system were stable at room temperature, and no aggregation or oriented attachment was observed [47, 48]. Jin [49, 50] found that in the synthesis of ZnO nanocrystals, the introduction of Mg dopants significantly influenced the growth of the host lattices by modifying the crystallographic phase of ZnO seeds, which eventually led to a dramatic shape evolution. A small amount of magnesium precursor

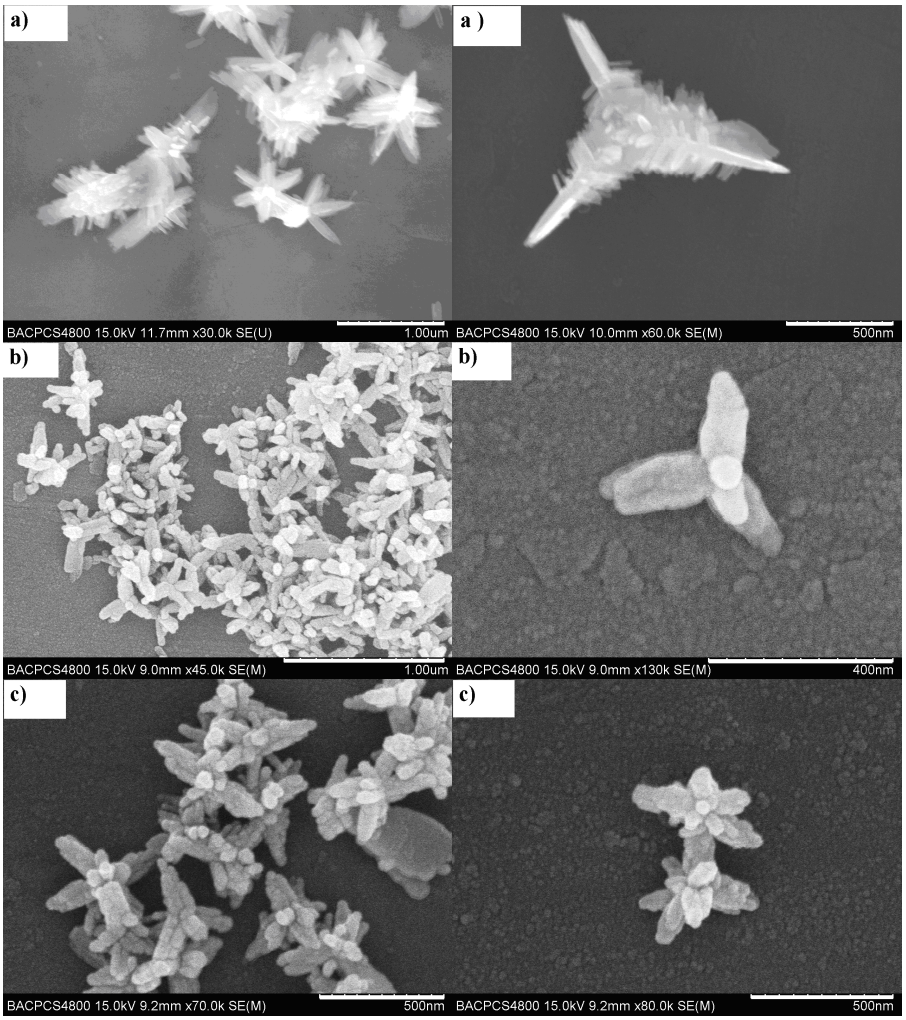

Figure 5. SEM images of as-synthesized ZnO whiskers under different water/cyclohexane ratios (growth time=10h; the water/cyclohexane ratio in a, b and c is 16:100, 8:100 and 5:100, respectively) [45]

(as low as 2 mol% $Mg(St)_2$ in the starting materials) significantly changed the morphology of the resulting nanocrystals, leading to tetrapods. Tetrapod-shaped nanocrystals were also obtained in the products from the 5 mol% and 10 mol% $Mg(St)_2$ reactions. For different dosages, the 5% $Mg(St)_2$ reaction had the maximum yield of high-quality ZnO nanotetrapods, i.e., as high as >95%.

In our work [51], magnesium acetate, zinc oxide, and stearic acid were used as reactants, and the obtained $Mg_xZn_{1-x}(St)_2$ in the first process was subsequently reacted with octodecyl alcohol or octadecylamine in the second process. Figure 6 shows that the obtained ZnO had the morphologies of nanotetrapods. The arm had a diameter of about 5 nm and a length of <50 nm.

Although most of the above-mentioned synthesis methods enable controlled growth of ZnO tetrapods, an easy scalable, cost-effective and facile synthesis method which can produce large amounts of size-controllable ZnO tetrapods is still an aspect in high demand. Compared with vapour-transport synthesis, ZnO tetrapods obtained from liquid reaction synthesis have smaller sizes; however, their yield and purity both decrease because of the lengthy washing process.

3. Growth Mechanism

The growth mechanism of ZnO tetrapods is still a subject of debate [52–55]. The factors affecting the morphologies of the tetrapod nanostructures and the possibility of controlling the tetrapod ZnO nanostructures during synthesis under suitable reaction conditions remain unclear. According to the differences in nanostructure formation mechanisms, the extensively used vapour transport process can be categorized as a catalyst-free vapour–solid (VS) process and a catalyst-assisted vapour–liquid–solid (VLS) process. References [56] and [57] give detailed descriptions of the nucleation rate calculation and growth model of ZnO nanoparticles via chemical vapour synthesis. The model successfully predicts the experimental yield of the reaction

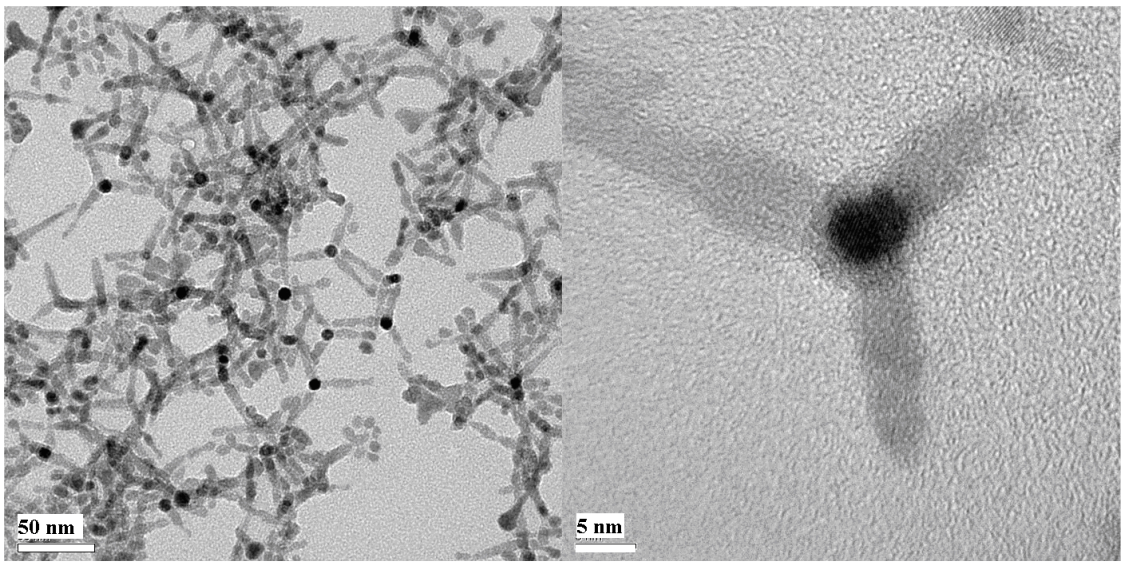

Figure 6. TEM images of ZnO whiskers by alcoholysis of $Mg_xZn_{1-x}(St)_2$ under 250℃

and shows that the kinetics of nucleation/growth of ZnO nanoparticles are probably very rapid when compared to the reaction of the oxidation of Zn vapour.

To date, three different growth mechanisms have been proposed for ZnO tetrapod formation by the catalyst-free VS process. Shiojiri and Kaito [58] prepared ZnO tetrapods by burning zinc metal in a gas mixture of 80% Ar and 20% O_2. The initially formed particles < 20 nm in size had the zincblende (ZB) structure. They became tetrapod-like crystals after rapid growth along four <111> directions perpendicular to the {111} or Zn faces. Then, WZ crystals were formed on their {111} faces by introducing stacking faults; they grew easily along their [0001] directions, and became ZnO tetrapods. Nishio et al. [59] proposed a growth model wherein ZnO tetrapods were formed from WZ multiple twins induced in a ZB nucleus, which only existed in high-temperature tetrapods and degenerated to multiple twins at room temperature. Iwanaga et al. [60, 61] reported ZnO tetrapods composed of core and legs with the same WZ structure. They proposed an octa-twin model and assumed that octahedral multiple inversion twins consisting of eight trigonal pyramidal crystals were formed first. The eight surfaces of the octahedron were alternately composed of the plus (0001) surface (+c) and minus (000, $\bar{1}$) surface (–c). The positively charged surfaces (+c) were likely to be terminated with Zn and were the favourable sites for attracting vapour species. During their growth, some twin boundaries cracked and the four legs grew only in the +c directions, resulting in the formation of tetrapods. Through experimentation, Dai [55] gave direct evidence on the existence of the octa-twin nucleus, strongly supported the octa-twin model. Figure 7 shows a pyramid formed by three {11, $\bar{2}$ 2} facets and one (0001) facet, and the octa-twin model composed of eight pyramidal inversion twin crystals.

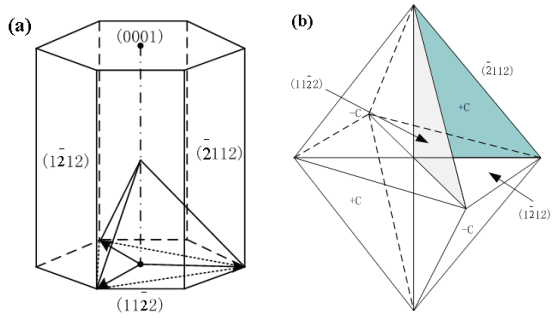

Figure 7. (a) A pyramid formed by three {11, $\bar{2}$ 2} facets and one (0001) facet, and (b) the octa-twin model composed of eight pyramidal inversion twin crystals

Other researchers believe that the growth mechanism of ZnO tetrapod and multipod nanostructures can be a self-catalyzed VLS process [62, 63] that generally involves two important steps: nucleation at the initial stage followed by epitaxial growth. The vapour of Zn or Zn suboxides (ZnO_x, $x < 1$) generated at the source region at high temperature were transferred to the low-temperature region, and then condensed into liquid droplets on the substrate. Consequently, the incoming O and Zn atoms were absorbed for nucleation and further growth of the ZnO nanostructure.

Overall, these growth models are inconsistent with one another. Thus, more work on morphological analysis, spectral measurements and theoretical calculations are needed to better explain the growth of ZnO tetrapods.

4. Application in Photovoltaic Devices

ZnO tetrapod architecture consisting of four rod-shaped structures joined at tetrahedral angles to a central core, has recently attracted much attention in the development of photovoltaic devices, because of the good electron trans-

port rates and electron collection in the three dimensional network built with them.

4.1 Usage of ZnO nanotetrapods as photoanodic materials in DSSCs

DSSCs are some of the most successful devices that exploit nanostructures to accomplish efficient solar-to-electric power conversion [64, 65]. Photoanodes are important components of DSSCs because of their functions in supporting dye molecules and transferring electrons. A high electron transport rate is required to reduce the electron–hole recombination rate and enhance the conversion efficiency. Although the most widely used photoanode material in DSSCs is mesporous TiO_2 films, various structures of ZnO are also being used for DSSC fabrication. The advantages of using ZnO over TiO_2 are its direct band gap (3.37 eV), higher exciton binding energy (60 meV) compared to TiO_2 (4 meV) and higher electron mobility (200 $cm^2\ V^{-1}\ s^{-1}$ for bulk material) over TiO_2 (0.1-4 $cm^2\ V^{-1}\ s^{-1}$). In addition, zinc oxide has a price advantage, and commercially available ZnO is cheaper than TiO_2 (the price of zinc oxide is below 2,000 US dollars per tonne, while the price of titanium dioxide is over 2,000 US dollars per tonne). The chemical stability of ZnO is, however, less than that of TiO_2, which was found to be problematic in the dye-adsorption procedure. Low electron injection efficiency from excited dye molecules to ZnO is also an obstacle to obtaining high efficiency [66-68].

ZnO nanotetrapods were deposited on Fluorine-doped tin oxide (FTO) glass substrate at 500 °C by a furnace method. The samples were used to combine with N-719 or N3 dyes to fabricate two kinds of DSSCs. Under optimal conditions, an AM 1.5 power conversion efficiency (η) of 0.40% was achieved for N3 immersed DSSC and 0.68% was achieved for N-719 immersed DSSC [69].

Chen [70] proposed a photoanode architecture for DSSCs based on ZnO nanotetrapods with a branched structure. The ZnO nanotetrapods were amenable to being assembled into a network with good mechanical strength. The network can maintain the characteristics of vertically aligned nanorod arrays by significantly reducing the numerous electron-hopping interjunctions in the porous nanoparticle films. For ZnO nanotetrapod film preparation, ZnO nanotetrapod powder was first dissolved in 1-butanol to form a sufficiently viscous paste. Then, the doctor blade technique was used to spread this paste onto an FTO substrate. After complete drying overnight in a vacuum oven at room temperature, the films were immersed in an ethanol solution of N-719 dye at 60 °C for 75 min to adsorb the dye sensitizer. Optimum performance of the ZnO nanotetrapod-based DSSCs, i.e., J_{sc} = 9.71 mA cm^{-2}, V_{oc} = 614 mV, FF = 0.55 and η = 3.27%, was achieved with a 31.1 μm thick photoanode.

Intensity modulated photocurrent/photovoltage spectroscopy (IMPS/IMVS) measurements have shown that the charge collection efficiency for the ZnO tetrapod films is much higher than that of the reference nanoparticle films [71, 72]. The size of ZnO tetrapod has a certain impact on the photoelectric conversion efficiency. The arm diameter determines the surface-to-volume ratio while the arm length-to-diameter ratio influences the packing density of the tetrapods. When micro-sized ZnO tetrapods were adopted, the limited specific surface area and packing density would restrict the performance of solar cell.

Chiu [73] reported a photoanode film composed of tetrapod-like ZnO nanoparticles, which were fabricated by a DC plasma method with D149 dye. The film provided good electron transport and light harvesting to achieve a conversion efficiency as high as 4.9%. The electron transport properties of the ZnO photoanode were also analysed by electrochemical impedance spectroscopy. The photoanode with a film thickness of 42.2 μm showed a good photovoltaic performance, with short circuit current density (J_{SC}), open circuit voltage (V_{OC}), fill factor (FF) and conversion efficiency(η) values of 12.4 mA cm^{-2}, 607 mV, 0.65 and 4.9%, respectively. The electrical impedance spectra provided information on the electron transport resistance from inside the ZnO photoanode, charge-transfer resistance related to electron recombination, chemical capacitance of the ZnO electrode, transport resistance of FTO and external circuits, effective electron lifetime, diffusion coefficient and diffusion length of ZnO photoanode. The effective electron diffusion coefficient and effective electron diffusion length for the 42.2 μm tetrapod-like ZnO DSSCs were 1.533 × 10^{-3} $cm^2\ s^{-1}$ and 45.57 μm, respectively.

Due to the low packing density, even with the relatively small ZnO nanotetrapods for the DSSC photoanodes, the specific surface for dye adsorption and the number of active sites for charge separation at the semiconductor/electrolyte interfaces remain low. Further increasing the nanotetrapod film thickness is a logical option, but it could cause cracks, thus affecting the charge collection. Another possibility is to introduce nanoparticles into the tetrapods' matrix. The ZnO tetrapod network works as a main electron transport passage while nanoparticles serve to increase the specific surface area and take part in the local charge transport.

Chen [74] also constructed ZnO nanotetrapods/SnO_2 composite photoanodes. The ZnO nanotetrapod network served as a global electron transport highway, and the nanoparticles increased the roughness factor and participated in the local charge transport. The optimal performance (η = 6.31%) was obtained at a 2:1 weight ratio of SnO_2:ZnO. When the composite photoanode design was later extended to flexible substrates, a cell efficiency of 4.91% was obtained. In addition, the ZnO nanotetrapods were replaced by large ZnO particles in the composite photoelectrode while maintaining the same ZnO:SnO ratio. The charge collection efficiency was found to be relatively lower under the working condition of one sun, which clearly demonstrated that the ZnO nanotetrapods support-

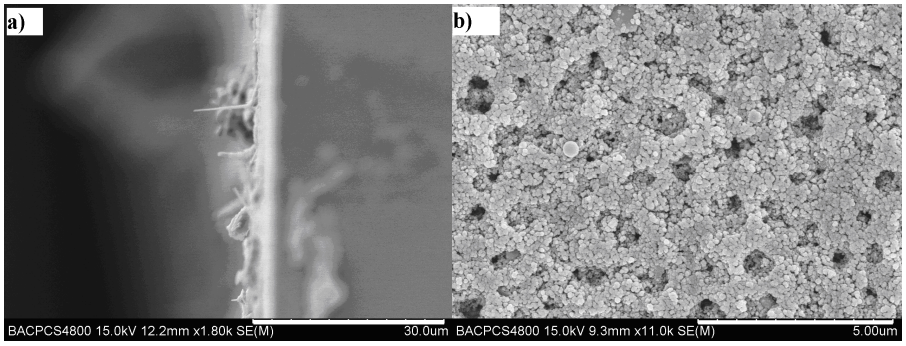

Figure 8. SEM cross-sectional (a) and top-view image (b) of ZnO tetrapods/TiO_2 photoanode fabricated via screen printing [75]

Device structure	PCE (%)	*Voc (V)*	*Jsc(mA cm^{-2})*	*FF*	Ref.
FTO+ZnO Tetrapods+N719	0.68	0.75	1.69	0.53	[69]
FTO+ZnO Tetrapods+N719	3.27	0.61	9.71	0.55	[70]
FTO+ZnO Tetrapods+D149	4.9	0.60	12.3	0.65	[73]
FTO+ZnO Tetrapods+SnO_2	6.31	0.66	16.30	0.59	[74]
FTO+ZnO Tetrapods+TiO_2+N3	1.87	0.74	4.74	0.53	[75]
FTO+ZnO Tetrapods+ CdS/CdSe	4.24	0.72	13.85	0.42	[76]
FTO+ZnO Tetrapods+ZnO NPs+N719	1.20	0.57	4.78	0.44	[77]
FTO+ ZnO Tetrapods+N719	4.78	0.66	10.79	0.67	[78]
FTO+ ZnO Tetrapods+N719	3.21	0.65	9.50	0.52	[79]
ITO/PEN+SnO_2 NPs+ ZnO Tetrapods+N719	4.91	0.68	12.00	0.60	[80]
FTO+ ZnO Tetrapods+D149	4.68	0.63	11.60	0.64	[81]

Table 1. Performance of DSSC based on ZnO tetrapods

ed faster electron transport in the composite film than the large ZnO particles, which was due to their structural difference. The large ZnO particles were separated from one another in the film, whereas for the ZnO nanotetrapods in the film, the 1D arm ensured easy directional charge transport, and the symmetrical branching structure guaranteed the formation of an excellent electron transport network.

A hybrid photoanode composed of ZnO and TiO_2 was fabricated on an FTO substrate using different techniques, including electrophoretic deposition, screen printing and colloidal spray coating [75]. Two kinds of ZnO, namely, ZnO tetrapods and ZnO nanorods, were adopted. Figure 8 shows the cross-sectional and top-view images of the ZnO tetrapods/TiO_2 photo-anode fabricated through screen printing. The ZnO tetrapods/TiO_2 composite film exhibited a uniform porous structure, which significantly increased the surface area and improved dye absorption. The DSSCs based on the screen printing-laminated TiO_2/ZnO tetrapods/TiO_2 photoanode had the highest efficiency of 1.87%, which was attributed to their uniform porous structure.

Cheng [76] fabricated composite photoanodes using ZnO tetrapods, CdS and CdSe quantum dots. The preliminary CdS layer was energetically favourable toward electron transfer and behaved as a passivation layer to diminish the formation of interfacial defects during CdSe synthesis. The ZnO tetrapods afforded an efficiently direct pathway instead of the interparticle hops when using conventional nanoparticles. An optimum CdS/CdSe quantum dot-sensitized ZnO tetrapod solar cell with an energy conversion efficiency as high as 4.24% was obtained. Table 1 displays performance characteristics of various ZnO tetrapods-based DSSCs.

4.2 Usage of ZnO nanotetrapods as electron acceptors in polymer solar cells

Interconnected tetrapods can form three-dimensional networks, which can provide a satisfactory transmission channel for electrons. Tetrapod-like semiconductor nanocrystals used as electron acceptors in polymer solar cells have been reported. Zhou [82] prepared tetrapodal nanocrystals of $CdSe_xTe_{1-x}$ with $x = 0$ (CdTe), 0.23, 0.53, 0.78, 1 (CdSe), which served as electron acceptors in a polymer solar cell based on MEH-PPV. V_{oc}, J_{sc} and η of the devices increased with increased Se content in the $CdSe_xTe_{1-x}$ nanocrystals. The solar cell based on the blend of tetrapodal CdSe nanocrystals and MEH-PPV (9:1, w/w) showed the highest η of 1.13% under AM 1.5, 80 mW cm^{-2}.

Sun [83] fabricated photovoltaic devices with CdSe nanotetrapods and poly (2- methoxy-5-(3′,7′-dimethyl-

octyloxy)-*p*-phenylenevinylene). The solar cells with CdSe nanotetrapods showed improved performance when compared with devices made from nanorod/polymer blends. The improvement was consistent with the enhanced electron transport perpendicular to the plane of the film. A solar power conversion efficiency of 1.8% was achieved under AM 1.5 illumination for a device containing 86 wt% nanotetrapods. Lee [84] synthesized CdSe, CdTe and type-II heterostructured CdTe/CdSe nanotetrapods, and then fabricated hybrid polymer solar cells with the blend of tetrapod nanocrystals and P3HT. The hybrid solar cell based on the blend of CdSe tetrapod nanocrystals and P3HT (6:1 weight ratio) showed the maximum power conversion efficiency of 1.03% under AM 1.5G condition. The CdTe and CdTe/CdSe tetrapod nanocrystals showed relatively poor photovoltaic performance because of the mismatch between the energy-band-level positions of P3HT and CdTe. Smita Dayal [85] fabricated hybrid polymer solar cells using CdSe nanotetrapods and a low-bandgap polymer, and the power conversion efficiency was 3.2%.

The application of tetrapod-like nanocrystals as electron acceptors in polymer solar cells has attracted considerable attention; however, the number of reports on the usage of ZnO tetrapods in polymer solar cells is limited. ZnO tetrapods prepared via a microemulsion-based hydrothermal method were introduced as electron acceptors to bulk heterojunctions to increase exciton separation, electronic transfer and effective collection. Two types of solar cells were fabricated with the structures of ITO/PEDOT:PSS/MEH-PPV:ZnO tetrapods/Al and ITO/PEDOT:PSS/MEH-PPV:ZnO tetrapods (1:1):PCBM/Al [86]. Figure 9 shows the morphology of the MEH-PPV: ZnO tetrapods: PCBM composite films. The dispersion of ZnO tetrapods in MEH-PPV was very poor and significant agglomeration existed. The expected homogeneous three-dimensional network structures were not formed, which caused the poor performance of solar cells. Figure 10 shows that ITO/PEDOT: PSS/MEH-PPV: ZnO tetrapods/Al had J_{sc} = 0.03 mA cm^{-2}, V_{oc} = 0.28 V and FF = 0.231. The conversion efficiency of the solar cell in which ZnO tetrapods were used as single electron acceptors was only 0.002%. Further analysis revealed that this solar cell had a high series resistance (R_s) of 3076 Ω cm^2, which directly caused the low J_{sc} and η. On the other hand, ITO/PEDOT: PSS/MEH-PPV: ZnO tetrapods: PCBM/Al had J_{sc} = 0.25 mA cm^{-2}, V_{oc} = 0.58 V and FF = 0.224. The efficiency slightly increased by combining PCBM as an electron acceptor.

Further studies should be conducted to improve the performance of hybrid polymer solar cells based on ZnO nanotetrapods further. Focus must be given to the following: 1) the appropriate amount of ZnO tetrapods, 2) improvement in the dispersion of ZnO tetrapods by surface functionalization to increase the interfacial surface area between organic and inorganic layers for charge separation, and 3) promotion of the formation of nanoscale

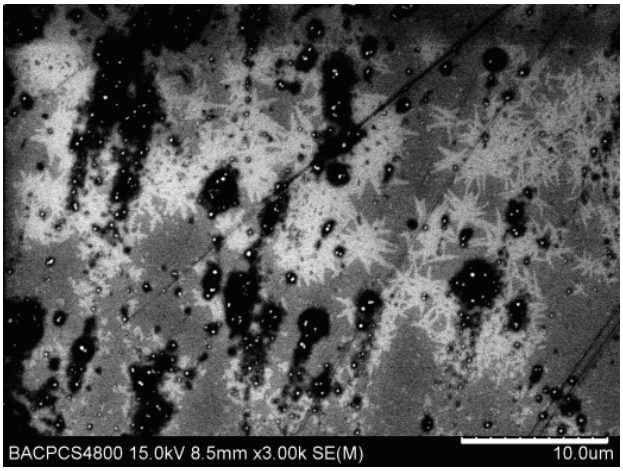

Figure 9. SEM of MEH–PPV: ZnO tetrapods: PCBM composite films [86]

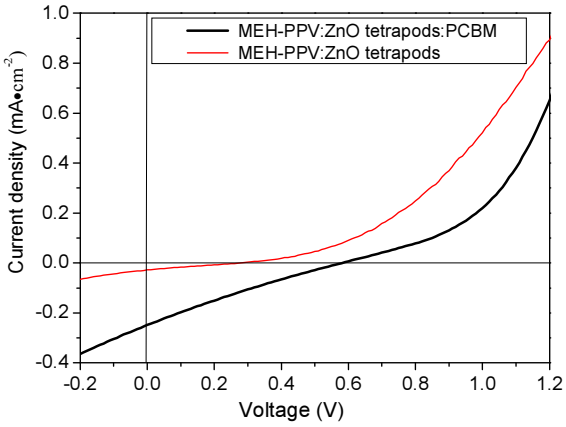

Figure 10. IV curves of two types of solar cells [86]

lengths and periodicity of each structure to enable charge separation and movement toward the appropriate electrode without recombination.

5. Discussions

Compared with liquid reaction processes, the vapour transport synthesis has great advantages: the preparation process is simple and ZnO tetrapods could be prepared on a large scale with high purity, and simultaneously without agglomeration formation. In all kinds of vapour-transport synthesis methods, the thermal evaporation process is the easiest to manipulate; however, the biggest drawback of this method is that the size of the tetrapod becomes too large when the control is poor. By introducing an inert gas under different flow rates, the nucleation and growth could be separated out to different temperature regions: nucleate at a high-temperature region and growth at a low-temperature region. Large amounts of tetrapod nuclei are formed and transported downstream to the colder area of the furnace. The growth can be quenched in a controlled fashion. Therefore, by using this inert gas flowing technique, one should be able to tailor the size and morphology of the tetrapods.

Controlled synthesis of ZnO tetrapods is very important for their successful application in solar cells. The ZnO tetrapods used in DSSC need a moderate arm length-to-diameter ratio to form a film with a high packing density as well as a high specific surface, which is beneficial for dye loading. The ZnO tetrapods produced by thermal evaporation with inert gas flowing can meet the basic requirements of DSSC, whereas the four arms of ZnO tetrapods produced by thermal evaporation are very smooth. In order to further increase the packing density and decrease the large cavities in ZnO tetrapods' network, branch growth could be tried to obtain secondary branching ZnO tetrapods [87]. The main backbone network of the ZnO tetrapods provides a highway for rapid electron transport and the branching expands the interface with the dyes for maximizing light absorption and charge separation at the interface, and therefore enhances device performance.

The branched ZnO tetrapods have a certain similarity with those ZnO tetrapods obtained by micro-emulsion combined with the thermal hydration method. With increased hydrothermal growth time to 10 h, secondary growth occurred, numerous tiny whiskers appeared on the arms and the branched ZnO tetrapods formed. The branched ZnO tetrapods are amenable to assembly into a highly connected network with excellent electron transport and mechanical strength, which once again placed more emphasis on the wet chemical method. Compared with vapour transport synthesis, wet chemical methods have a demanding operation process requiring steady hands and the utmost patience, especially in the later washing and drying stages, which often introduce impurities and causes agglomeration. However, wet chemical methods have unique advantages over the morphology and size control.

Further reduction of the size of ZnO tetrapods remains a very attractive topic, especially in the application of ZnO tetrapods in a hybrid polymer solar cell whose active layer is in the range of 100-200 nm because of the low-charge carrier mobility of the polymer. Small ZnO tetrapods with a size of less than 20 nm can form a three-dimensional network for efficient electron collection and transportation, and will not affect the thickness and morphology of the active layer. Although there is still the potential for size reduction with vapour transport synthesis, the production of ZnO nanotetrapods with a size smaller than 20 nm via this method has not been reported. The nonhydrolytic alcoholysis route could produce ZnO nanotetrapods less than 20 nm. Most important of all, surface modification could be suitably completed in the preparation process or the post-processing stage. Surface modification can tune the optical and electrical properties of ZnO nanotetrapods and further endow them with new functions. Moreover, surface modification could be used to immobilize and assemble function moieties such as C_{60} on the surface of ZnO tetrapods via carboxylic linkage [88], which will enable new applications and phenomena in solar cells. Obviously, if the yield can be further increased, then wet chemical methods combined with surface modification have great potential for development.

6. Conclusions

One important advantage of tetrapods over other nanocrystalline geometric forms is that their four arms easily connect to each other to form a porous network. Branched tetrapods' nanostructures provide improved electron extraction in photovoltaic devices compared with 1D nanorod structures or bulk materials; however, further improvements on the performance of photovoltaic devices based on ZnO nanotetrapods are still required. We suggest that further research should focus on: reduction of the nanotetrapods' size while increasing the yield, surface modification of ZnO nanotetrapods to enhance their solubility in organic solvents and increase their compatibility with the organic phase, and element doping to regulate the bandgap and conductivity. The application of ZnO tetrapods in solar cells is at its initial stages, and factors such as the dosage, dispersion and surface functionalization need to be explored.

7. Acknowledgements

The work was supported by the National Natural Science Foundation of China (11475017), a CSC Scholarship (201407095076) and the Fundamental Research Funds for the Central Universities (2013JBM094).

8. References

[1] Gimenez A J, Yáñez-Limón J M (2011) Seminario. ZnO-Paper based photoconductive UV sensor. J. Phys. Chem. C 115: 282–287.

[2] Gupta S K, Joshi A, Kaur M (2010) Development of gas sensors using ZnO nanostructures. J. Chem. Sci. 122:57–62.

[3] Yao B D, Chan Y F, Wang N (2002) Formation of ZnO nanostructures by a simple way of thermal evaporation. Appl. Phys. Lett. 81:757-759.

[4] Fan Z Y, Lu J G (2005) Zinc oxide nanostructures: synthesis and properties. J. Nanosci. Nanotechnol. 10: 1561-1573.

[5] Wang Z L (2004) Zinc oxide nanostructures: growth. properties and applications. J. Phys.: Condens. Matter. 16:R829–R858.

[6] Singh J, Kumar P, Late D J, Singh T, More M A, Joag D S, Tiwari R S, Hui K S, Srivastava O N (2012) Optical and field emission properties in different nanostructures of ZnO. Dig. J. Nanomater. Bios. 7: 795-806.

[7] Zhong Y, Djurisic A B, Hsu Y F, Wong K S, Brauer G, Ling C C, Chan W K (2008) Exceptionally long exciton photoluminescence lifetime in ZnO tetrapods. J. Phys. Chem. C 112:16286-16295.

[8] Niu L N, Fang M, Jiao K, Tang L H, Xiao Y H, Shen L J, Chen J H (2010) Tetrapod-like zinc oxide

whisker enhancement of resin composite. J. Dent. Res. 89:746-750.

[9] Jin X, Götz M, Wille S, Kumar Mishra Y, Adelung R, Zollfrank C (2013) A novel concept for self-reporting materials: stress sensitive photoluminescence in ZnO tetrapod filled elastomers. Adv. Mater. 25:1342–1347.

[10] Antoine T, Mishra Y K, Trigilio J, Triwari V, Adelun R, Shukla D (2012) Prophylactic. therapeutic and neutralizing effects of zinc oxide tetrapod structures against herpes simplex virus type-2 infection. Antiviral Res. 96:363-375.

[11] Jin X, Strueben J, Heepe L, Kovalev A, Mishra Y K, Adelung R, Gorb S N, Staubitz A (2012) Joining the un-joinable: adhesion between low surface energy polymers using tetrapodal ZnO linkers. Adv. Mater. 24: 5676-5680.

[12] Fan Z, Wang D, Chang P C (2004) ZnO nanowire field-effect transistor and oxygen sensing property. Appl. Phys. Lett. 85:5923-5925

[13] Zhang Z X, Yuan H J, Gao Y, Wang J X, Liu D F, Shen J, Liu L F, Zhou W Y, Xie S S, Wang X, Zhu X, Zhao Y C, Sun L F (2007) Large-scale synthesis and optical behaviors of ZnO tetrapods. Appl. Phys. Lett. 90:153116.

[14] Leung Y H, Kwok W M, Djurišić A B, Phillips D L, Chan W K (2005) Time-resolved study of stimulated emission in ZnO tetrapod nanowires. Nanotechnology 16:579-582.

[15] Djurišić A B, Kwok W M, Leung Y H, Chan W K, Phillips D L, Lin M S, Gwo S (2006) Ultrafast spectroscopy of stimulated emission in single ZnO etrapod nanowires. Nanotechnology 17:244-249.

[16] Newton M C, Warburton P A (2007) ZnO tetrapod nanocrystals. Mater. Today 10:50-54.

[17] Zhou Z W, Liu S K, Gu L X (2001) Studies on the strength and wear resistance of tetrapod-shaped ZnO whisker–reinforced rubber composites. J. Appl. Polym. Sci. 80:1520-1525.

[18] Pang Q, Zhao L J H, Liang C, Qin A, Wang J (2013) Preparation and characteristics of nanotetrapods CdSe-polymer hybrid solar cells. Bull. Mater. Sci. 36:1161–1164.

[19] Meulenkamp E A (1998) Synthesis and growth of ZnO nanoparticles. Phys. Chem. B 102:5566–5572.

[20] Polarz S, Roy A, Merz M, Halm S, Schrçder D, Schneider L, Bacher G, Kruis F E, Driess M (2005) Chemical vapor synthesis of size-selected Zinc Oxide nanoparticles. Small 1:540-552.

[21] Kruis F E, Fissan H, Peled A (1998) Synthesis of nanoparticles in the gas phase for electronic. optical and magnetic applications—a review. J. Aerosol. Sci. 29:511–535.

[22] Kurda A, Hassan Y, Ahmed N (2015) Controlling diameter. length and characterization of ZnO nanorods by simple hydrothermal method for solar cells. World J. Nano. Sci. Eng. 5:34-40. doi: 10.4236/wjnse.2015.51005.

[23] Mani G K, Rayappan J B B (2014) Novel and facile synthesis of randomly interconnected ZnO nanoplatelets using spray pyrolysis and their room temperature sensing characteristics. Sensor Actuat. B-Chem. 198:125–133.

[24] Unalan H E, Hiralal P, Rupesinghe N, Dalal S, Milne W I, Amaratunga G A J (2008) Rapid synthesis of aligned zinc oxide nanowires. Nanotechnology. 19:255608 doi:10.1088 / 0957-4484/19/25/255608

[25] Lupana O, Chowa L, Chaid G (2009) A single ZnO tetrapod-based sensor. Sensor Actuat. B-Chem. 141:511–517.

[26] Rackauskas S, Mustonen K, Järvinen T, Mattila M, Klimova O, Jiang H, Tolochko O, Lipsanen H, Kauppinen E I, Nasibulin A G (2012) Synthesis of ZnO tetrapods for flexible and transparent UV sensors. Nanotechnology 23:095502.

[27] Yan H, He R, Pham J, Yang P (2003) Morphogenesis of one-dimensional ZnO nano- and microcrystals. Adv. Mater. 15:402–405.

[28] Bengisu M (2001) Engineering Ceramics. Springer-Verlag New York.

[29] Zhou Z W, Deng H, Yi J, Liu S K (1999) A new method for preparation of zinc oxide whiskers. Mater. Res. Bull. 34:1563-1567.

[30] Delaunay J J, Kakoiyama N, Yamada I (2007) Fabrication of three-dimensional network of ZnO tetratpods [sic] and its response to ethanol. Mater. Chem. Phys. 104:141–145.

[31] Wang P, Yan L T, Wu H P, Zhou C Y, Si W J (2009) Effect of process parameters on the preparation T-ZnOw. Journal of Materials Science & Engineering 27: 75-77.

[32] Qiu Y F, Yang S H (2007) ZnO nanotetrapods: controlled vapor-phase synthesis and application for humidity sensing. Adv. Funct. Mater. 17: 1345–1352.

[33] Carotta M C, Cervi A, di Natale V, Gherardi S, Giberti A, Guidi V, Puzzovio D, Vendemiati B, Martinelli G, Sacerdoti M, Calestani D, Zappettini A, Zha M, Zanotti L (2009) ZnO gas sensors: a comparison between nanoparticles and nanotetrapods-based thick films. Sens. Actuators. B 137: 164–169.

[34] Bacsa R R, Dexpert-Ghys J, Verelst M, Falqui A, Machado B, Bacsa W S, Chen P, Zakeeruddin S M, Graetzel M, Serp P (2009) Synthesis and structure–property correlation in shape-controlled ZnO nanoparticles prepared by chemical vapor synthesis and their application in dye-sensitized solar cells. Adv. Funct. Mater. 19: 875–886.

[35] Singh J, Srivastava A, Tiwari R, Srivastava O (2005) Nucleation and growth of catalyst-free zinc oxide

nanostructures. J. Nanosci. Nanotechnol. 5:2093-2098.

[36] Choopuna S, Tabata H, Kawai T (2005) Selfassembly ZnO nanorods by pulsed laser deposition under argon atmosphere. J. Cryst. Growth 274:167-172.

[37] Chen Z, Shan Z W, Cao M S, Lu L, Mao S X (2004) Zinc oxide nanotetrapods. Nanotechnology 15:365–369.

[38] Yang B, Wang C Y, Li D F, Yin F, Chen Y Q, Jie X W (2010) Effects of impurity elements on morphology of zinc oxide product prepared by oxidation of zinc vapor. Materials Review 24:53-57.

[39] Wang F Z, Ye Z Z, Ma D W, Zhu L P, Zhuge F (2005) Novel morphologies of ZnO nanotetrapods. Mater. Lett. 59:560– 563

[40] Wisitsoraat A, Pimtara I, Phokharatkul D, Jaruwongrangsee K, Tuantranont A (2010) Zinc oxide nanopolypods synthesized by thermal evaporation of carbon nanotubes and zinc oxide mixed powder. Current Nanoscience 6:1-9.

[41] Bhoomanee C, Hongsith N, Wongrat E, Choopun S, Wongratanaphisan D (2011) Effect of solution on growth of zinc oxide tetrapod by thermal oxidation technique. Chiang Mai J. Sci. 38:187-192.

[42] Wu Y P, Zhang X H, Xu F C, Zheng L S, Kang J Y (2009) A hierarchical lattice structure and formation mechanism of ZnO nano-tetrapods. Nanotechnology 20:325709.

[43] Zhang X H, Xie S Y, Jiang Z Y, Xie Z X, Huang R B, Zheng L S, Kang J Y, Sekiguchi T (2003) Microwave plasma growth and high spatial resolution cathodoluminescent spectrum of tetrapod ZnO nanostructures. J. Solid State Chem. 173:109–113

[44] Jiang J Y, Li Y F, Tan S W, Huang Z Y (2010) Synthesis of zinc oxide nanotetrapods by a novel fast microemulsion-based hydrothermal method. Mater. Lett. 64:2191-2193.

[45] Ai X D, Yan L T, Liu Y C, Li T X, Dou S Y, Dai C A (2012) Preparation and influencing factors of ZnO whisker by hydrothermal microemulsion process. Advanced Materials Research 528:193-196.

[46] Li X C, He G H, Xiao G K, Liu H J, Wang M (2009) Synthesis and morphology control of ZnO nanostructures in microemulsions. J. Colloid. Interface Sci. 333:465–473.

[47] Chen Y F, Kim M, Lian G D, Johnson M B, Peng X G (2005) Side reactions in controlling the quality. yield. and stability of high quality colloidal nanocrystals. J. Am. Chem. Soc. 127:13331-13337.

[48] Wang Q L, Yang Y F, He H P, Chen D D, Ye Z Z, Jin Y Z (2010) One-step synthesis of monodisperse in-doped ZnO nanocrystals. Nanoscale Res. Lett. 5:882–888.

[49] Yang Y F, Jin Y Z, He H P, Wang Q L, Tu Y (2010) Dopant-induced shape evolution of colloidal nanocrystals: the case of zinc oxide. J. Am. Chem. Soc. 132:13381-13394.

[50] Jin Y Z, Ren Y P, Cao M T, Ye Z Z (2012) Doped colloidal ZnO nanocrystals. J. Nanomater. 985326.

[51] Liu Y C (2014) Interface modification and active layer design in polymer solar cells. [dissertation] Beijing. BJTU: School of Sciences.

[52] Dai Y, Zhang Y, Li Q K, Nan C W (2002) Synthesis and optical properties of tetrapod-like zinc oxide nanorods. Chem. Phys. Lett. 358:83-86.

[53] Roy V A L, Djurisic A B, Chan W K, Gao J, Lui H F, Surya C (2003) Luminescent and structural properties of ZnO nanorods prepared under different conditions. Appl. Phys. Lett. 83:141-143.

[54] Yu W D, Li X M, Gao X D (2004) Self-catalytic synthesis and photoluminescence of ZnO nanostructures on ZnO nanocrystal substrates. Appl. Phys. Lett. 84:2658-2660.

[55] Dai Y, Zhang Y, Wang Z L (2003) The octa-twin tetraleg ZnO nanostructures. Solid State Commun. 126:629-633.

[56] Reuge N, Bacsa R, Serp P, Caussat B (2009) Chemical vapor synthesis of zinc oxide nanoparticles: experimental and preliminary modeling studies. J. Phys.Chem. C 113:19845-19852.

[57] Ali M, Winterer M (2010) Influence of nucleation rate on the yield of ZnO nanocrystals prepared by chemical vapor synthesis. J. Phys. Chem. C 114:5721-5726.

[58] Shiojiri M, Kaito C (1981) Structure and growth of ZnO smoke particles prepared by gas evaporation technique. J. Cryst. Growth 52:173-177.

[59] Nishio K, Isshiki T, Kitano M, Shiojiri M (1997) Structure and growth mechanism of tetrapod-like ZnO particles. Phil. Mag. A. 76:889-904.

[60] Fujii M, Iwanaga H, Ichihara Takeuch M S (1993) Structure of tetrapod-like ZnO crystals. J. Cryst. Growth 128:1095-1098.

[61] Iwanaga H, Fujii Takeuch M S (1993) Growth model of tetrapod zinc oxide particle. J. Cryst. Growth 134:275-280.

[62] Zheng K, Xu C X, Zhu G P, Li X, Liu J P, Yang Y, Sun X W (2008) Formation of tetrapod and multipod ZnO whiskers. Physica E 40:2677–2681.

[63] Wang F Z, Ye Z Z, Ma D W, Zhu L P (2005) Rapid synthesis and photoluminescence of novel ZnO nanotetrapods. J. Cryst. Growth 274:447-452.

[64] O'Regan B, Gratzel M (1991) A low-cost. higheffi-ciency solar cell based on dye-sensitized colloid TiO_2 Films. Nature 353:737-740.

[65] Nazeeruddin M K, Kay A, Rodicio I, Humphry-Baker R, Mueller E, Liska P, Vlachopoulos N, Graetzel M (1993) Conversion of light to electricity by cis-X2bis (2,2'-bipyridyl-4,4'-dicarboxylate)ruthenium (II) charge-transfer sensitizers (X =

Cl-, Br-, I-, CN-, and SCN-) on nanocrystalline titanium dioxide electrodes. J. Am. Chem. Soc. 115:6382-6390.

[66] Chergui Y, Nehaoua N, Mekki D E (2011) Comparative Study of Dye-Sensitized Solar Cell Based on ZnO and TiO_2 Nanostructures. Solar Cells - Dye-Sensitized Devices. Prof. Leonid A. Kosyachenko (Ed.), ISBN: 978-953-307-735-2, InTech.

[67] Quintana M, Edvinsson T, Hagfeldt A, Boschloo G (2007) Comparison of dye-sensitized ZnO and TiO_2 solar cells: studies of charge transport and carrier lifetime. J. Phys. Chem. C 111:1035-1041.

[68] Chandiran A K, Abdi-Jalebi M, Nazeeruddin M K, Grätzel M (2014) Analysis of electron transfer properties of ZnO and TiO_2 photoanodes for dyesensitized solar cells. ACS Nano 8:2261–2268. DOI: 10.1021/nn405535j

[69] Lin T W (2010) Synthesis of ZnO tetrapod nanocrystals on FTO glass substrate by furnace method and their application of dye-sensitized solar cells. [dissertation] Taiwan. NTOU: Institute of Optoelectronic Sciences.

[70] Chen W, Zhang H F, Hsing I M, Yang S H (2009) A new photoanode architecture of dye sensitized solar cell based on ZnO nanotetrapods with no need for calcinations. Electrochem. Commun. 11:1057–1060.

[71] Chen W, Qiu Y C, Yang S H (2012) Branched ZnO nanostructures as building blocks of photoelectrodes for efficient solar energy conversion. Phys. Chem. Chem. Phys. 14:10872–10881.

[72] Oekermann T, Zhang D, Yoshida T, Minoura H (2004) Electron transport and back reaction in nanocrystalline TiO_2 films prepared by hydrothermal crystallization. J. Phys. Chem. B 108:2227-2235.

[73] Chiu W H, Lee C H, Cheng H M, Lin H F, Liao S C, Wu J M, Hsieh W F (2009) Efficient electron transport in tetrapod-like ZnO metal-free dye-sensitized solar cells. Energy Environ. Sci. 2:694–698.

[74] Chen W, Qiu Y, Zhong Y, Wong K S, Yang S (2010) High-efficiency dye-sensitized solar cells based on the composite photoanodes of SnO2 nanoparticles/ZnO nanotetrapods. J. Phys. Chem. A 114:3127–3138.

[75] Yan L T, Wu F L, Peng L, Zhang L J, Li P J, Dou S Y, Li T X (2012) Photoanode of dye-sensitized solar cells based on a ZnO/TiO_2 composite film. International Journal of Photoenergy. Article ID 613969.

[76] Cheng H M, Huang K Y, Lee K M, Yu P, Lin S C, Huang J H, Wu C G, Tang J (2012) High-efficiency cascade CdS/CdSe quantum dot-sensitized solar cells based on hierarchical tetrapod-like ZnO nanoparticles. Phys. Chem. Chem. Phys. 14:13539–13548.

[77] Hsu Y F, Xi Y Y, Yip C T, Djuriši A B, Chan W K (2008) Dye-sensitized solar cells using ZnO tetrapods. J. Appl. Phys. 103:083114.

[78] Lee C H, Chiu W H, Lee K M, Yen W H, Lin H F, Hsieh W F, Wu J M (2010) The influence of tetrapodlike ZnO morphology and electrolytes on energy conversion efficiency of dye-sensitized solar cells. Electrochimica Acta 55:8422-8429.

[79] Yuejun F (2012) Study of ZnO nanotetrapods based solar cell. [dissertation] KunMing. Guangxi University.

[80] Chen W, Qiu Y, Yang S (2010) A new ZnO nanotetrapods/SnO2 nanoparticles composite photoanode for high efficiency flexible dye-sensitized solar cells. Phys. Chem. Chem. Phys. 12:9494–9501.

[81] Lee K M, Chiu W H, Hsu C Y, Cheng H M, Lee C H, Wu C G (2012) Ionic liquid diffusion properties in tetrapod-like ZnO photoanode for dye-sensitized solar cells. J. Power Sources 216:330-336.

[82] Zhou Y, Li Y C, Zhong H Z, Hou J H, Ding Y Q, Yang C H, Li Y F (2006) Hybrid nanocrystal/polymer solar cells based on tetrapod-shaped CdSexTe1−x nanocrystals. Nanotechnology 17:4041-4047.

[83] Sun B Q, Marx E, Greenham N C (2003) Photovoltaic devices using blends of branched CdSe nanoparticles and conjugated polymers. Nano Lett. 3:961-963

[84] Lee H, Kim S, Chung W S, Kim K, Kim D (2011) Hybrid solar cells based on tetrapod nanocrystals: the effects of compositions and type II heterojunction on hybrid solar cell performance. Sol. Energy Mater. Sol. Cells 95:446–452.

[85] Dayal S, Kopidakis N, Olson D C, Ginley D S, Rumbles G (2010) Photovoltaic devices with a low band gap polymer and CdSe nanostructures exceeding 3% efficiency. Nano Lett. 10:239-242.

[86] Zhang L N (2011) The studies of preparation of polymer/ZnO hybrid solar cell. Thesis. [dissertation] Beijing. BJTU: School of Sciences.

[87] Qiu Y, Yan K, Deng H, Yang S (2012) Secondary branching and nitrogen doping of ZnO nanotetrapods: building a highly active network for photoelectrochemical water splitting. Nano Lett. 12: 407-413.

[88] Liu D, Wu W, Qiu Y, Yang S, Xiao S, Wang Q Q, Ding L, Wang J (2008) Surface functionalization of ZnO nanotetrapods with photoactive and electroactive organic monolayers. Langmuir 24:5052-5059.